CFD Simulation of a Wing-In-Ground-Effect UAV

IOP Conf. Series: Materials Science and Engineering **370** (2018) 012006 doi:10.1088/1757-899X/370/1/012006

CFD Simulation of a Wing-In-Ground-Effect UAV

C T Lao[1] and E T T Wong[2]

[1] Interdisciplinary Division of Aeronautical and Aviation Engineering, The Hong Kong Polytechnic University, Hong Kong

[2] Department of Mechanical Engineering, The Hong Kong Polytechnic University, Hong Kong

[1] jack.lao@connect.polyu.hk
[2] mmttwong@connect.polyu.hk

Abstract. This paper reports a numerical analysis on a wing section used for a Wing-In-Ground-Effect (WIG) unmanned aerial vehicle (UAV). The wing geometry was created by SolidWorks and the incompressible Reynolds-averaged Navier-Stokes (RANS) equations were solved with the Spalart–Allmaras turbulence model using CFD software ANSYS FLUENT. In FLUENT, the Spalart-Allmaras model has been implemented to use wall functions when the mesh resolution is not sufficiently fine. This might make it the best choice for relatively crude simulations on coarse meshes where accurate turbulent flow computations are not critical. The results show that the lift coefficient and lift-drag ratio derived excellent performance enhancement by ground effect. However, the moment coefficient shows inconsistency when the wing is operating in very low altitude - this is owing to the difficulty on the stability control of WIG vehicle. A drag polar estimation based on the analysis also indicated that the Oswald (or span) efficiency of the wing was improved by ground effect.

1. Introduction

In the long history of aerodynamic research, it was proven that a lifting body operates proximately to a physical boundary (or ground) has greater aerodynamic efficiency than when it operates in freestream. 'Ground effect' is an enhanced aerodynamic performance phenomenon of a lifting body, which is evident while a lifting body operating in close proximity to the ground [1].

A Wing-In-Ground-Effect (WIG) vehicle needs some forward velocity to produce lift dynamically and the principal benefit of operating a wing in ground effect is to reduce its lift-dependent drag. The basic design principle is that the closer the wing operates to an external surface such as the ground, said to be in ground effect, the more efficient it becomes. As sea surface provides a more stable boundary in comparing to dry land, WIG vehicle is a suitable and eco-friendly solution on high speed marine transportation purpose. Some of researches have discussed the service limitations and capabilities of WIG vehicle and summarized that is a possible solution of niche transportation in multi-island countries such as Malaysia, the Philippines and Caribbean area [2][3].

In this paper, a CFD simulation was carried out to analyze the aerodynamic characteristics of a wing used in a WIG UAV. The analysis examines the performance of the wing in both freestream and ground effect air flow. The analysis results are significantly important for future WIG vehicle and WIG UAV developments in terms of flight dynamics and control.

2. Theory

In the early century, ground effect is also called as 'cushion effect' since it act as an air cushion which support the aircraft while landing. Theoretically, ground effect is caused by the following physical phenomena [4]:

1. Since the downward airflow movement (or downwash) is blocked by the boundary, more air molecules stay under the wing bottom surface and the pressure on these area increases. Due to this, the airflow spanwise vector would be strengthened and the wing effective span enlarges. Furthermore, the wing aspect ratio increases relatively with effective span, hence, lift force raises.

2. Due to the airflow blockage, wingtip vortex would not acuminate as the aircraft in freestream. When the vortex flows reach to the boundary, it would stop to distribute around the wingtip. The reduction of strength of wingtip vortex also reduces the induced drag and downwash.

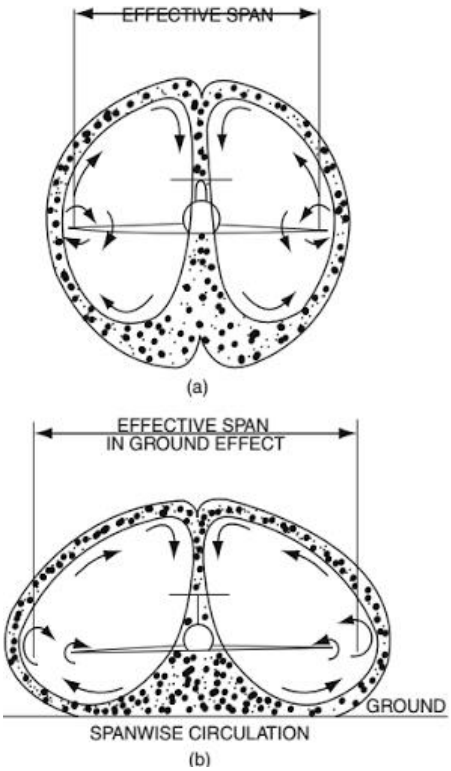

Figure 1. Flow illustration of wing with and without ground effect [4]

3. Research methodology

A wing prototype (Fig. 2) was constructed using SolidWorks and it was exported to ANSYS for creating a mesh and computational domain. To save the computer resources, only single side of the wing would be examined. The wing is a Lippisch style reversed delta wing which has a root chord of 300mm, a tip chord of 75mm and 300mm span. Airfoil shape for this wing is Clark-Y.

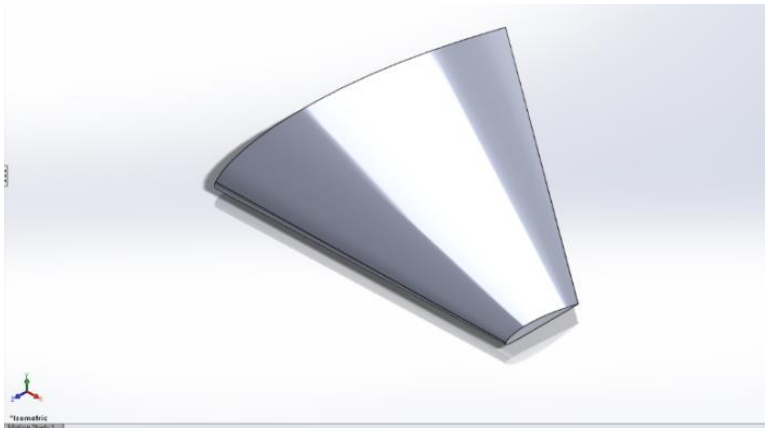

Figure 2. Wing geometry

The CFD simulation was carried out on ANSYS FLUENT, and the incompressible Reynolds-averaged Navier-Stokes (RANS) equations were solved with the Spalart–Allmaras (S-A) turbulence model at the Reynolds number of 2.05×10^5 (based on the averaged chord length of wing chord)[5]. The Spalart-Allmaras model is a relatively simple one-equation model that does not require the calculation of a length scale related to the local shear layer thickness. The Spalart-Allmaras model was designed specifically for aerospace applications involving wall-bounded flows and has been shown to give good results for boundary layers subjected to adverse pressure gradients. The lift, drag and moment coefficients and lift-drag ratio (aerodynamic efficiency) were estimated in the freestream flow of 16 m/s for various angles of attack, viz. 0, 5, 10, 15, and 20 degrees.

For ground effect analysis, the operating altitude of the wing is defined as the ratio between height above ground and mean chord length (h/c). With lower h/c number, the wing is closer to the ground. The height is defined as the distance between the mean quarter chord and ground. In this analysis, the operating altitude of the wing in terms of height-chord ratio would be 0.5 (93.75mm above ground), 1.0 (187.5mm) and 1.5 (281.25mm). The ground effect can be negligible for h/c > 1 and the wing in this altitude can be considered as operating in freestream air.

4. Governing equations and turbulence model

Similar to the most cases of CFD, ANSYS FLUENT is governed by Reynolds-averaged Navier–Stokes (RANS) equations with various turbulence models which depend on the application.

The general form of continuity equation is written as:

$$\frac{\partial u_i}{\partial x_i} = 0 \tag{1}$$

And the momentum equation is written as:

$$\rho \bar{u}_j \frac{\partial \bar{u}_i}{\partial x_i} = \rho \bar{f}_i + \frac{\partial}{\partial x_j}\left[-\bar{p}\delta_{ij} + \mu\left(\frac{\partial \bar{u}_i}{\partial x_j} + \frac{\partial \bar{u}_j}{\partial x_i}\right) - \rho\overline{u'_i u'_j}\right] \tag{2}$$

In terms of turbulence model selection, various researches figured out that Spalart–Allmaras turbulence model would be the most suitable one for handling WIG effect problems due to result accuracy and integrity [6][7].

The one equational model is written as:

$$\frac{\partial \tilde{v}}{\partial t} + u_j \frac{\partial \tilde{v}}{\partial x_j} = C_{b1}[1 - f_{t2}]\tilde{S}\tilde{v} + \frac{1}{\sigma}\{\nabla[(v + \tilde{v})\nabla\tilde{v}] + C_{b2}|\nabla\tilde{v}|^2\} - \left[C_{w1}f_w - \frac{C_{b1}}{\kappa^2}f_{t2}\right]\left(\frac{\tilde{v}}{d}\right)^2 + f_{t1}\Delta U^2 \quad (3)$$

Where the terms involved are:

$$v_t = \tilde{v}f_{v1};\ f_{v1} = \frac{X^3}{X^3 + C^3{}_{v1}};\ \mathrm{X} := \frac{\tilde{v}}{v};\ \tilde{S} \equiv \mathrm{S} + \frac{\tilde{v}}{\kappa^2 d^2}f_{v2},\ f_{v2} = 1 - \frac{X}{1 + Xf_{v1}};\ f_w = g\left[\frac{1 + C^6{}_{w3}}{g^6 + C^6{}_{w3}}\right]^{1/6};$$

$$\mathrm{g} = \mathrm{r} + C_{w2}(r^6 - r);\ \mathrm{r} \equiv \frac{\tilde{v}}{\tilde{S}\kappa^2 d^2};\ f_{t1} = C_{t1}g_t \exp\left(-C_{t2}\frac{w_t{}^2}{\Delta U^2}\left[d^2 + g_t{}^2 d_t{}^2\right]\right);\ f_{t2} = C_{t3}\exp(-C_{t4}X^2);$$

$$\mathrm{S} = \sqrt{2\Omega_{ij}\Omega_{ij}}$$

The rotation tensor is given by:

$$\Omega_{ij} = \frac{1}{2}\left(\partial u_i / \partial x_j - \partial u_j / \partial x_i\right) \quad (4)$$

The constants used in the analysis are:

$\sigma = \frac{2}{3};\ C_{b1} = 0.1355;\ C_{b2} = 0.622;\ \kappa = 0.41;\ C_{w1} = \frac{C_{b1}}{\kappa^2} + \frac{1 + C_{b2}}{\sigma^2};\ C_{w2} = 0.3;\ C_{w3} = 2;\ C_{v1} = 7.1;$
$C_{t1} = 1;\ C_{t2} = 2;\ C_{t3} = 1.1;\ C_{t4} = 2$

5. Mesh And Boundary Conditions

Once the CAD file was exported to ANSYS, a box of dimensions 0.5m × 0.5m × 1m is created to cover the wing which acts as a fluid chamber or a virtual wind tunnel. A subtract Boolean condition is applied where the box is target body and the wing is the tool body.

To simplify the procedure on CFD, except the minimum grid size, all meshing parameters would be the default values in ANSYS. All models have been meshed with tetrahedral, unstructured grids since the mesh can automatically be generated with default values, which reduces the complexity to create the computational domain. For all meshing files, the numbers of elements are at least 500,000 but not beyond the upper mesh limit (512,000 elements for ANSYS 17.1 Academic)

The boundary conditions were defined for various sections – these include the inlet, outlet, ground and sidewall. The inlet velocity would be 16 m/s, and the outlet gauge pressure would be 0 Pa. The turbulent viscosity ratio is 10 and the modified turbulent viscosity is 0.000146 m^2/s for all simulation. A moving wall conditions is applied to simulate the ground. It is a no-slip wall and slides along x direction with the same velocity of inlet flow. Finally, a symmetrical boundary condition was set on the sidewall to achieve a zero shear condition.

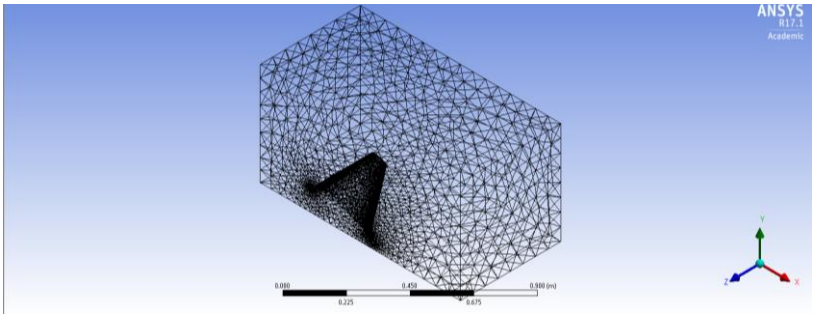

Figure 3. Geometry mesh

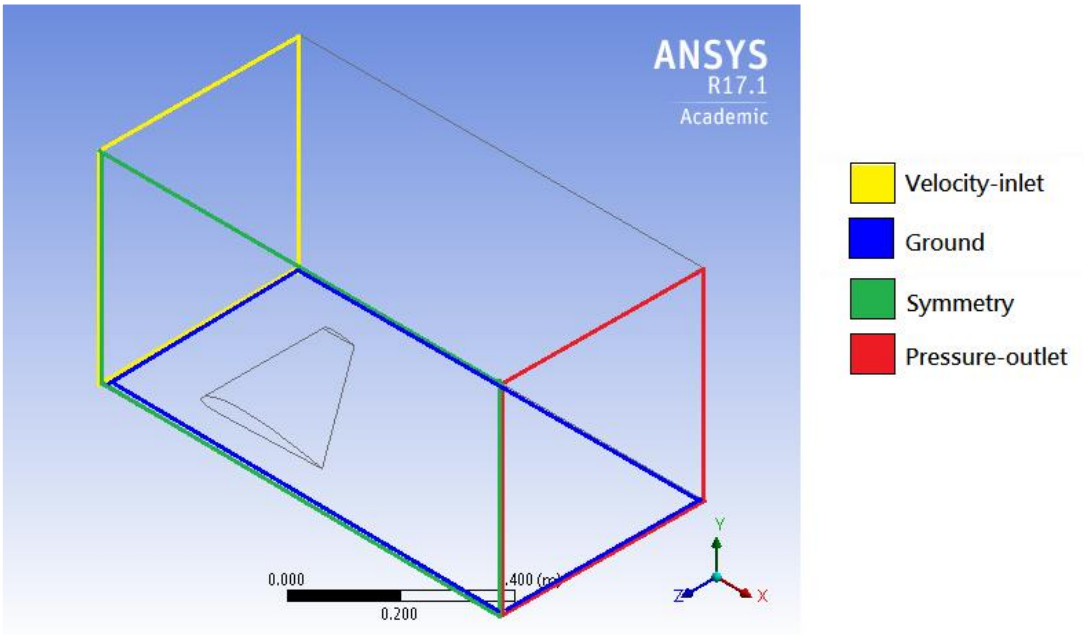

Figure 4. Boundary conditions

6. Result and discussion

Referring to Fig. 5, which showed that the enhancement by ground effect in terms of lift coefficient. The lift coefficients before stall when the wing flies at 0.5 height-chord ratio, is 1.85 times of it flies at 1.5 h/c. Also, the lift gradient is greater when the wing flies with assisting by ground effect. In terms of drag coefficient (fig. 6), the differences are not significant when the wing flies at different flight level unless in high angles of attack.

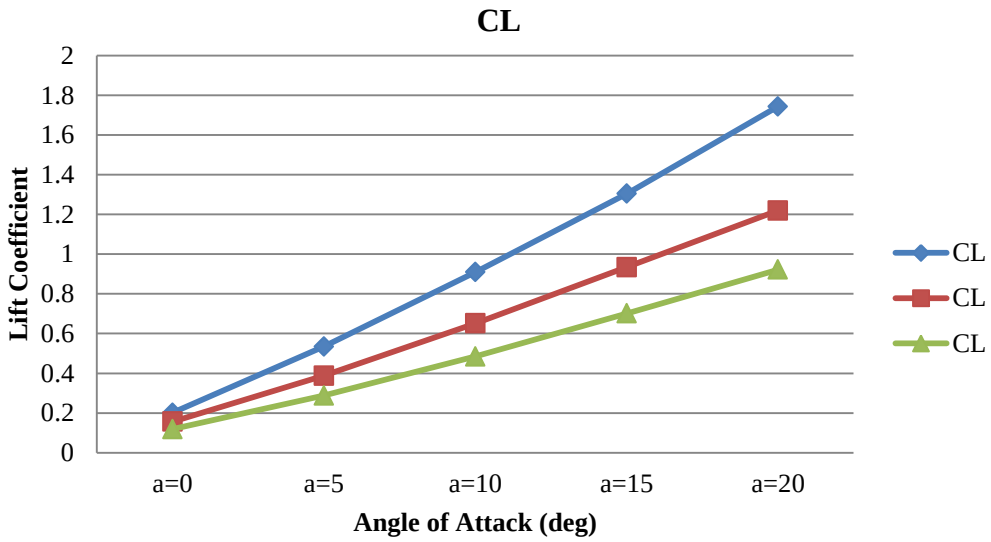

Figure 5. Lift coefficient

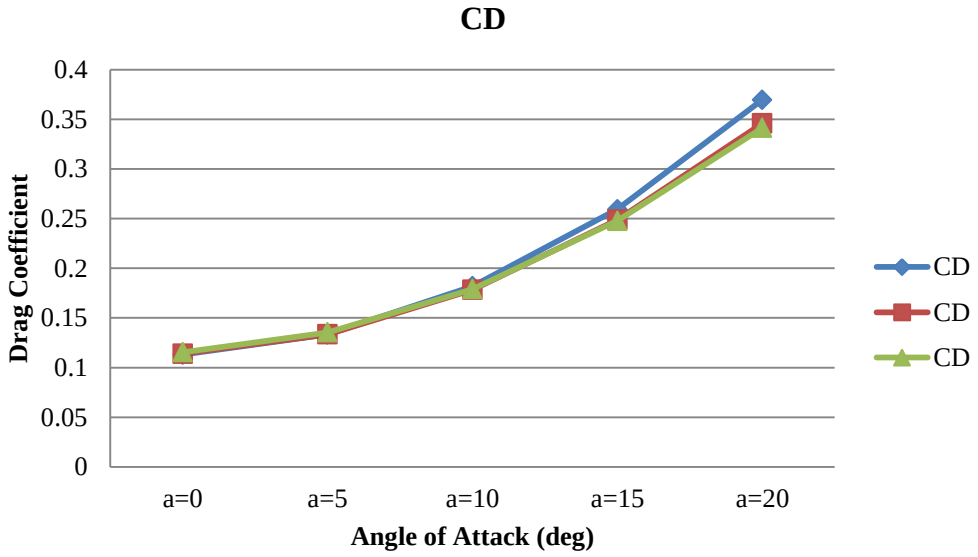

Figure 6. Drag coefficient

In terms of moment coefficient (Fig. 7), it is not consistent in different operation altitude as the wing flies in freestream air. It means the pitching moment will change significantly with very small operating altitude change. When the wing operates relatively closer to the ground, the moment coefficient is more sensitive with the wing angle of attack. This shows the difficulty on maintaining the longitudinal stability while operating a WIG vehicle.

Combining the results of lift and drag coefficients, it can be summarized that the lift-drag ratio (fig. 8) is greatly enhanced by ground effect.

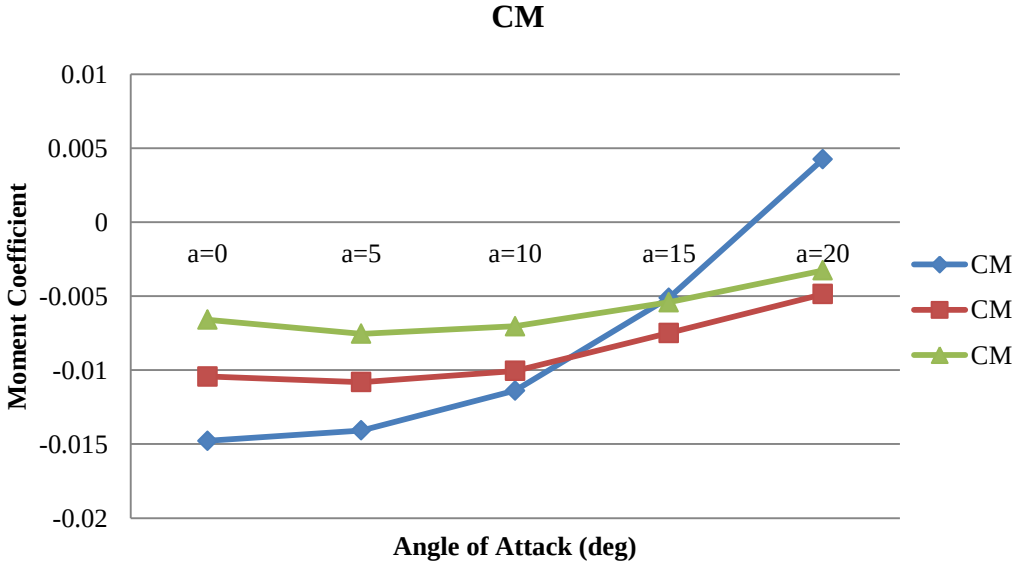

Figure 7. Moment coefficient

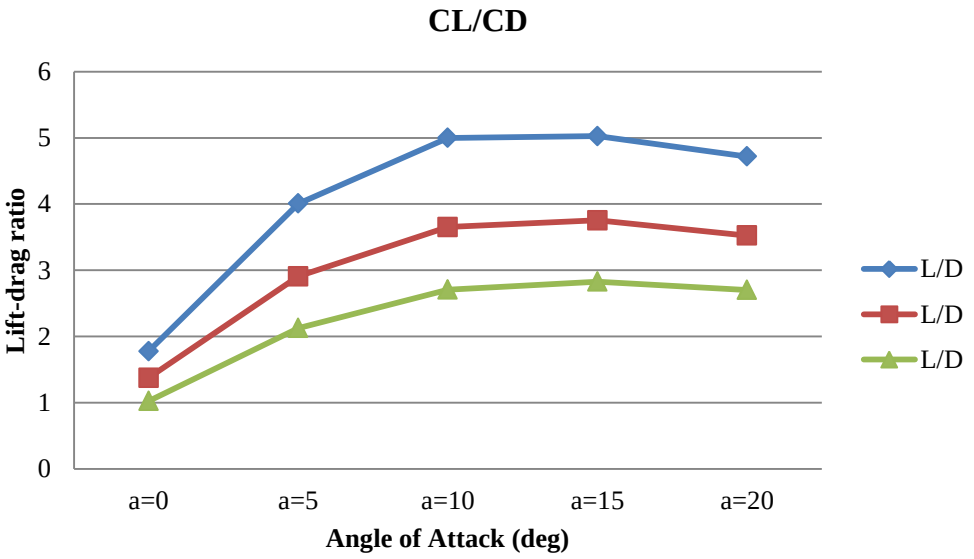

Figure 8. Lift-drag ratio

7. Mesh independence study

To validate the results generated, a mesh independence study was carried out for the wing angle of attack in 15 degree at various altitude. The numbers of element in this study are fairly close to 300,000 (ultra-coarse mesh), 400,000 (coarse) and 500,000 (fine) which are adjusted by changing minimum grid size. The result in lift-drag ratio are shown in the figure 9.

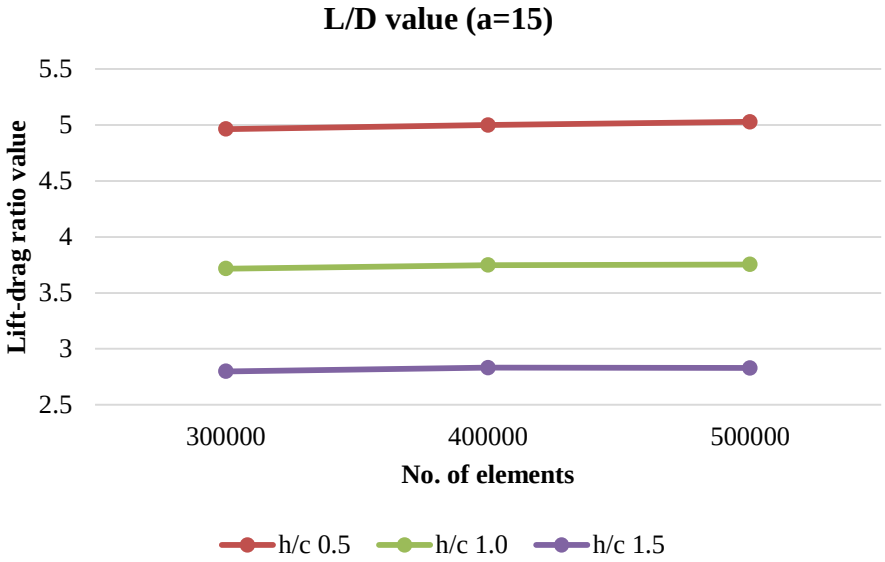

Figure 9. Variation of lift-drag ratio at variated mesh size

The study shows that the variation in terms of lift-drag ratio values have no significant changes at coarser mesh. The mean difference in result between ultra-coarse mesh and fine mesh is about 1% which is acceptable for the simulation. It was proven that the results obtained in this simulation are valid which have no dependency with number of mesh element.

8. Drag polar estimation

Drag is one of aerodynamic forces applied to the wing and it includes two major parts: parasite drag and induced drag. Drag polar is one of major aerodynamic considerations in terms of wing design which is the major factor of induced drag. The drag polar (K) of the wing is affected by the wing aspect ratio (AR) and the Oswald efficiency (e).

The drag coefficient (C_D) can be explained as:

$$C_D = C_{D,0} + K{C_L}^2, where\ K = \frac{1}{\pi eAR} \tag{5}$$

For the first derivative of C_D to ${C_L}^2$:

$$\frac{dC_D}{d{C_L}^2} = K \tag{6}$$

$$\frac{d{C_L}^2}{dC_D} = \pi eAR \tag{7}$$

For π and AR are constant for the wing, hence:

Table 1. Drag polar estimation.

	K (Drag polar)	**e (Oswald efficiency)**
h/c=0.5	0.085761	1.160459
h/c=1.0	0.158474	0.628004
h/c=1.5	0.312145	0.318834

In the CFD simulation, the wings of WIG vehicle were designed at low aspect ratio (3.2 for this design). A major drawback of this wing is that the induced drag coefficient plays the major role in total drag coefficient. The estimated results showed the drag polar in h/c=0.5 was only 27.4% of it in the freestream, which means the induced drag was reduced with aid of ground effect.

9. Concluding remarks

The increase of the numerically calculated lift coefficient in the ground mode was 85% when compared to the lift coefficient in a freestream. The estimated results also showed that the Oswald efficiency of the wing was improved by ground effect. These positive numerical results indicate that wider application of WIG UAV has a great potential. However, before building a real WIG UAV model, one should also study the problem of flight stability and control. Hence further works have been planned on the fabrication and flight testing of the model UAV.

References

[1] Cui E and Zhang X 2010 Ground Effect Aerodynamics *Encyclopedia of Aerospace Engineering* ed R Blockley and W Shyy (Hoboken: John Wiley & Sons, Ltd.) Cheapter 18 245-256
[2] Yang W and Czysz P A 2011 WIG craft serves niche transportation needs *World Review of Intermodal Transportation Research* **3** 395-406
[3] Taylor G K 2002 Are You Missing The Boat? The Ekranoplan in the 21ST Century - Its Possibilities and Limitations
[4] Yun L, Bliault A and Doo J 2010 WIG craft and ekranoplan *Ground Effect Craft Technology* (New York: Springer) 26-27
[5] ANSYS 2013 ANSYS Fluent Theory Guide
[6] Genua E 2009 A CFD Investigation into Ground Effect Aerodynamics
[7] Qu Q, Lu Z, Liu P and Agarwal R K 2014 Numerical study of aerodynamics of a Wing-in-Ground-Effect craft *Journal of Aircraft*